Separation of Krypton and Xenon by Selective Permeation

S. A. STERN

and

S. M. LEONE

Dept. of Chemical Engineering and Materials Science
Syracuse University, Syracuse, N.Y. 13210

The objective of this investigation was to study the separation of krypton and xenon from nuclear reactor atmospheres by selective permeation through silicone rubber capillaries. Effective permeability coefficients for pure krypton xenon, nitrogen, and oxygen were determined between 0 and 40°C and at pressure differences across the capillary walls (Δp) of up to 3.45×10^5 N/m^2 (50 psi). The silicone rubber capillaries had an O.D. of 635 μm (0.025 in.) and an I.D. of 305 μm (0.012 in.), and were pressurized externally. The effective permeability coefficients decreased with increasing Δp due to the elastic deformation of the capillaries, in general agreement with a deformation analysis of thick-walled elastic tubes.

Gas separation studies were made with a Kr-Xe-N_2-O_2 mixture in a permeator containing a bundle of silicone rubber capillaries. The permeator had an effective permeation area of 0.480 m^2 (5.165 ft^2) at a packing density of 4132 m^2/m^3 permeator volume (1260 ft^2/ft^3), and was operated in a countercurrent mode. The separation studies were conducted at −10 and 20°C and at three Δp values. The separation achieved in the permeator at Δp's of 1.38×10^5 N/m^2 (20 lb/in.^{2}) and 2.07×10^5 N/m^2 (30 lb/in.^{2}) was in good agreement with that predicted from a theoretical model of a permeation stage with countercurrent flow. At 3.45×10^5 N/m^2 (50 lb/in.^{2}), the separation approached that predicted from a "perfect mixing" model. This behavior probably was due to local collapses of the capillaries at weak spots in their walls, as was evidenced also by a sharp increase in the axial pressure drop inside the capillaries.

SCOPE

The increasing use of nuclear energy to augment the conventional sources of energy has resulted in a strong demand for improved safety in the operation of nuclear reactors. One of the possible dangers in the operation of a nuclear reactor is the accidental release of radioactive ^{85}Kr and $^{133\text{-}135}$Xe to the atmosphere within a reactor containment dome. The radioactive krypton and xenon must then be separated and safely disposed of before the reactor can be further used (Belter, 1963; Blumkin et al., 1966). In 1963, Belter stated that this problem "could be the controlling factor in building large power reactors in populated areas." In the aftermath of the accident at the Three Mile Island nuclear power plant near Harrisburg, Pa., Belter's statement shows remarkable foresight.

Several techniques of separating radioactive krypton and xenon from mixtures with air and other gases have been studied in recent years. These studies were aimed at the development of a separation plant that is sufficiently compact to be easily transported to the scene of an accident. The removal of radioactive krypton and xenon is also of interest for the decontamination of the off-gas from plants that process spent reactor fuels and of the cover gas of a liquid-metal-cooled fast breeder reactor.

One of the most promising techniques for the separation of krypton and xenon is the selective permeation of gases through nonporous polymeric membranes. Rainey, Carter, and Blumkin (1971) at Oak Ridge National Laboratory have made a detailed investigation of this separation process, using silicone rubber membranes in sheet form as permeation barriers. These investigators found that the capital investment costs of conventional adsorption and extraction processes were somewhat lower than those of the permeation process. However, selective permeation may be better suited for the removal of krypton and xenon from reactor atmospheres because it is safer and potentially more reliable than other separation processes.

The objective of the present work was to determine the feasibility of separating krypton and xenon from air by permeation through silicone rubber capillaries. The use of capillaries would greatly decrease the size of permeator equipment, because a very large permeation area can be packed in a small volume. Additionally, capillary (or "hollow fiber") permeators are sturdy and relatively easy to build. Consequently, such permeators are particularly well suited for the construction of mobile permeation plants. The studies reported below were performed in a single permeation stage. The enhancement of the separation effect in a multistage permeation cascade will be reported in a following publication. All measurements were conducted with nonradioactive gases, but the possible effects of radiation on the permeation processes are discussed briefly.

Correspondence concerning this paper should be addressed to S. A. Stern.

0001-1541-80-4187-0881-$01.05.

CONCLUSIONS AND SIGNIFICANCE

Krypton and xenon can be effectively separated from mixtures with oxygen and nitrogen by selective permeation through silicone rubber capillaries. In the present study, the extent of separation of a Kr-Xe-N_2-O_2 mixture achieved in a single permeation stage at different temperatures, pressures, and stage cuts was in satisfactory agreement with that predicted from a suitable theoretical model. The measurements were performed in a capillary permeator which was operated in the countercurrent mode. A similar agreement was reported earlier for the separation of an O_2-N_2-Ar mixture, the permeator being operated in the cocurrent mode (Stern, Onorato, and Libove, 1977). Consequently, existing theoretical models can be used with some confidence to describe the performance of capillary permeators, at least such as tested in this work. All theoretical calculations assumed that the permeability coefficients of the components of the gas mixtures were the same as those of the pure components. This assumption appears to be adequate for mixtures of gases which exhibit a low solubility in silicone rubber.

Practical permeator modules using silicone rubber capillaries as permeation barriers are easily constructed and can be operated at elevated pressures. Such devices resemble shell-and-tube heat exchangers, and are best operated with the gas pressure applied outside the capillaries, or shell-side. This mode of operation is preferable because any accidental overpressurization will only result in a collapse of the capillaries, which can resume their normal shape once the excess pressure is relieved. By contrast, if the gas pressure is applied inside the capillaries (i.e., tube-side), such an accident may cause a rupture of the capillaries and a mixing of the high and low-pressure gas streams. Note, however, that external pressurization may result in a maldistribution of the high-pressure (unpermeated) gas stream if the permeator is not properly designed.

The highest pressure difference across capillary walls, Δp, at which separation can be performed effectively with the silicone rubber capillaries used in the present work appears to be about 3.45×10^5 N/m^2 (50 lb/in.^{2}). At this Δp, local collapses of the capillaries ("pinching") tend to lower the separation efficiency due to a decrease in the effective capillary length and an increase in the axial pressure drop. This limitation in Δp, and thus in the permeation flux, is mitigated by the large membrane area which can be packed in a capillary permeator. For example, a capillary packing density corresponding to 4132 m^2 of membrane area per m^3 of permeator volume (1260 ft^2/ft^3) was employed in the present work. This membrane area is about five times larger than obtainable in a permeator with sheet membranes.

The permeator modules described above can be improved in two ways. First, the membrane area per unit permeator volume can be further increased by the use of smaller bore capillaries, or "hollow fibers." Modules with hollow fibers will probably operate more efficiently with internal, or tube-side, pressurization because of a more beneficial pressure profile (Antonson et al., 1977). Second, Japanese investigators have recently proposed methods of increasing the degree of separation achievable in a single permeation stage (Kimura et al., 1973; Ohno et al., 1976-1978). These methods involve the use of more than one type of polymeric membrane for a given separation process, as well as of gas recycling techniques. The above improvements will reduce both the operating and capital investment costs of the membrane separation process under consideration.

SEPARATION OF KR AND XE BY SELECTIVE PERMEATION

Permeation of Gases through Elastic Capillaries

The rate of permeation G of a pure gas through the wall of a homogeneous, thick-walled polymer capillary or tube, which is pressurized externally, is given by the relation:

$$G = \frac{2\pi \mathcal{L} \bar{P} (p_O - p_I)}{\ln (R_O/R_I)} \tag{1}$$

where $\bar{P}$ is the mean permeability coefficient for the gas-capillary system; $\mathcal{L}$ is the length of the capillary; p_O and p_I are the gas pressures on the outer and inner surfaces of the capillary, respectively ($p_O > p_I$); and R_O and R_I are the outer and inner radii of the capillary, respectively. Eq. 1 applies to elastic capillaries as well as to rigid capillaries, provided that: (a) R_O, R_I, and $\mathcal{L}$ are the actual dimensions, taking into account the deformations due to gas pressure, and (b) the homogeneity of the material, in regard to its permeability coefficient $\bar{P}$, is not destroyed by the inhomogeneity of the elastic strains. Eq. 1 may be written in terms of the initial dimensions of the capillaries, i.e. those of the unstressed capillaries, provided that a correction term f_1 is also included to compensate for the use of the incorrect dimensions:

$$G = f_1 \frac{2\pi \ell \bar{P} (p_O - p_I)}{\ln (r_O/r_I)} \tag{2}$$

where ℓ, r_O, and r_I are the length, outer and inner radii, respectively, prior to the application of the pressures p_O and p_I. Eqs. 1 and 2 then yield:

$$f_1 = \frac{\mathcal{L} \ln (r_O/r_I)}{\ell \ln (R_O/R_I)} \tag{3}$$

The value of the dimensionless term f_1 depends on the elastic properties of the capillaries, their initial geometry, and the magnitude of the external and internal pressures. To find the values of f_1 analytically requires an elastic analysis of the stressed capillary. This analysis should be based on finite, rather than infinitesimal elasticity theory. An analysis of this type was made by Stern, Onorato, and Libove (1977) for the case in which p_O is variable, p_I = 1 atm, and the capillary material is incompressible

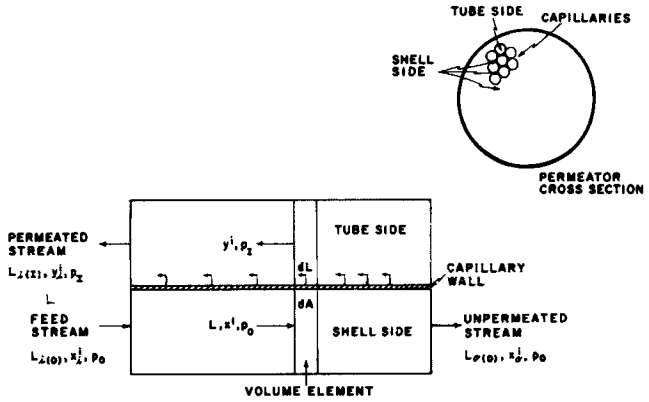

Figure 1. Diagram of permeation stage with countercurrent flow.

and initially isotropic. According to the analysis, f_1 is calculated from:

$$f_1 = (1 + e_a)\frac{\ln(n)}{\ln(nq/Q)} \tag{4}$$

where

$$e_a = \frac{1}{\sqrt{q}} - 1 \tag{5}$$

$$Q = \sqrt{n^2q^2 + (1 - n^2)\sqrt{q}} \tag{6}$$

and *where* $q = R_I/r_I$, the contraction of the inner radius of the capillary; $Q = R_O/r_O$, the contraction of the outer radius; and $n = r_I/r_O$, the ratio of internal-to-external radii of the unstressed capillary. The gauge pressure p for which an f_1 value applies is given by:

$$p = \frac{2}{3}E\frac{1}{\sqrt{q}}\left(1 - \frac{q}{Q}\right) \tag{7}$$

where E is Young's modulus. In using Eq. 7, it is practical to regard q as the independent variable. The equations show that the application of external pressure has two effects on an elastic capillary, to increase its O.D./I.D. ratio and to increase its length $\mathscr{L}$. The first effect causes a decrease in the effective permeability of the capillary by increasing its wall thickness, whereas the second effect increases the permeability by increasing the permeation area. Except for very thick-walled capillaries or tubes ($n < 0.25$), the initial effect of applied pressure is to reduce the permeability of an elastic capillary to a value below what it would be for a rigid one. This is due to the fact that at first the external pressure tends to increase the O.D./I.D. ratio faster than it increases the capillary length $\mathscr{L}$. Therefore, the denominator in Eq. 1 increases faster than the numerator. When the external pressure becomes sufficiently large, the increase in $\mathscr{L}$ predominates and the permeability increases. For very thick-walled capillaries, the lengthening effect predominates from the beginning causing the permeability to increase for any applied pressure.

The mean permeability coefficient $\bar{P}$ has been found to be an exponential function of the temperature at constant pressure difference across the capillary wall:

$$\bar{P} = P' \exp(-E_p/RT) \tag{8}$$

where E_p is the energy of activation for permeation; R is the universal gas constant; T is the absolute temperature; and P' is a constant. Eq. 8 is usually valid over a limited range of temperatures.

The local rate of permeation of the i-th component of a gas mixture can also be expressed by Eqs. 1 and 2, except that: (a) the pressures p_O and p_I must be replaced by the partial pressures x^ip_O and y^ip_I, where x^i and y^i are the mole fractions of component i at any given point outside and inside the capillary, respectively; and, (b) the mean permeability coefficient $\bar{P}^i$ for component i must be used. If the solubility of the components of the mixture in the polymer is sufficiently low (e.g., in Henry's law limit) the components can be assumed to permeate independently of each other. The mean permeability coefficient for the pure component can then be substituted for $\bar{P}^i$.

Separation of Gas Mixtures

The components of a gas mixture permeate through a nonporous polymeric membrane at different rates; permeation can therefore be used as a gas separation technique. Theoretical models of gas separation in a single permeation stage (i.e., in a permeator module containing a membrane in either sheet or tubular form) have been reviewed by Stern (1972, 1976), and by Hwang and Kammermeyer (1977). The various factors which affect the separation of a gas mixture in a permeation stage and the required membrane area have also been discussed. One of the controlling factors is the flow pattern of the high-pressure (unpermeated) and low-pressure (permeated) gas streams in the stage. The most efficient flow pattern, which yields the highest separation and requires the smallest membrane area, is the one where these streams flow countercurrently to each other (Walawender and Stern, 1972; Blaisdell and Kammermeyer, 1973). A countercurrent flow pattern was used for this reason in the present study. The analysis of gas separation in a permeation stage with countercurrent flow is summarized below for the case of a multicomponent feed.

Reference is made to the permeation stage illustrated in Figure 1, which is self-explanatory. The membrane consists of a bundle of capillaries, and a cross-section of a capillary wall is shown in the figure. It is assumed that no axial mixing occurs in either the high- or low-pressure gas streams, and that the pressure drop outside and inside the capillaries is negligible. Taking a material balance over a differential element of the stage dz yields the following relation for the i-th component of the mixture:

$$Lx^i = (L - dL)(x^i - dx^i) + \frac{2\pi(Ndz)\bar{P}^{*i}(x^ip_O - y^ip_I)}{\ln(r_O/r_I)} \tag{9}$$

where L is the local flow rate of the high-pressure (unpermeated) stream outside the capillaries; $\bar{P}^{*i}$ $(= \bar{P}^if_1)$ is the effective permeability coefficient for the stressed capillaries; N is the number of capillaries in the stage; and the other symbols are as defined before. Eq. 9 can be rearranged in the following form (neglecting second-order differentials):

$$\frac{dx^i}{dz} = \left[\frac{2\pi N\bar{P}^{*i}(x^ip_O - y^ip_I)}{\ln(r_O/r_I)} - x^i\frac{dL}{dz}\right]\frac{1}{L} \tag{10}$$

The change in the local flow rate of the high-pressure stream equals the total permeation rate:

$$\frac{dL}{dz} = \frac{2\pi N}{\ln(r_O/r_I)}\sum_{i=1}^{m}\bar{P}^{*i}(x^ip_O - y^ip_I) \tag{11}$$

where m is the number of components.

By combining Eqs. 10 and 11 one obtains:

$$\frac{dL}{dx^i} = \frac{L}{\left[\alpha_{ij}(x^i - y^ip_r)\Big/\sum_{i=1}^{m}\alpha_{ij}(x^i - y^ip_r)\right] - x^i} \tag{12}$$

where $p_r = p_I/p_O$, and $\alpha_{ij} = \bar{P}^{*i}/\bar{P}^{*j}$; α_{ij} is the ideal separation factor for any component i relative to some reference component j. Next, total and component material balances from some arbitrary point in the stage to the stage outlet yield the relation:

$$y^i = \frac{Lx^i - L_{i(O)}(1 - \theta)x_o^i}{L - L_{i(O)}(1 - \theta)} \tag{13}$$

where the subscripts "i" and "o" designate the boundaries of the permeation stage at the inlet and outlet of the high-pressure (unpermeated) stream, respectively. The flow rate of the high-

pressure stream at the stage inlet (i.e., the feed rate) is thus designated $L_{t(O)}$; the flow rate of the low-pressure stream at its outlet (i.e., the permeated product rate) is $L_{t(I)}$; and the stage cut is $\theta = L_{t(I)}/L_{t(O)}$. The subscripts "$I$" and "$O$" designate, as before, the low- and high-pressure streams inside and outside the capillaries, respectively.

A new dimensionless variable (Blaisdell and Kammermeyer, 1973)

$$L' = L/[L_{t(O)}(1 - \theta)] \tag{14}$$

is now introduced in Eqs. 12 and 13, which become:

$$\frac{dL'}{dx^i} = \frac{L'}{\left[\alpha_{ij}(x^i - y^i p_r)\Big/\sum_{i=1}^{m}\alpha_{ij}(x^i - y^i p_r)\right] - x^i} \tag{15}$$

and

$$y^i = \frac{L'x^i - x_0^i}{L' - 1} \tag{16}$$

where x_0^i is the mole fraction of the i-th component in the high-pressure stream at the stage outlet.

Eqs. 15 and 16 are used to determine the composition of the two product streams, i.e., the mole fractions x_0^i and y_1^i. The following initial and boundary conditions are employed in these calculations:

Initial conditions at the high-pressure stage outlet (for each component):

$$x^i = x_0^i \text{ and } y^i = y_0^i \text{ at } L' = 1$$

Values of x_0^i are first assumed, and the corresponding y_0^i's are calculated from the ratio of transport equations:

$$\frac{y_0^i}{y_0^j} = \alpha_{ij}\frac{x_0^i p_O - y_0^i p_I}{x_0^j p_O - y_0^j p_I}, \quad i \neq j \tag{17}$$

where the superscript "j" designates a specified reference component. Substituting this relation in the summation $\sum_{i=1}^{m} y_0^i = 1$ yields,

$$y_0^j + \sum_{\substack{i=1\\ i\neq j}}^{m}\frac{\alpha_{ij}x_0^i y_0^j p_O}{x_0^j p_O + (\alpha_{ij} - 1)\,y_0^j p_I} = 1 \tag{18}$$

where y_0^j is obtained from Eq. 18, being the only variable, and y_0^i is then calculated from Eq. 17.

Boundary conditions at the high-pressure stage inlet:

$$x^i = x_1^i \text{ at } L' = 1/(1 - \theta)$$

where x_1^i is the mole-fraction of component i in the feed to the stage.

For a given stage cut θ, the composition of the low-pressure (permeated) stream, in terms of y_1^i's, can be determined by trial-and-error from Eqs. 15 and 16, starting with the assumed compositions x_0^i. The calculation, using x_1^i as an iteration factor, must match the specified feed composition x_1^i to the desired convergence criterion. The length $\mathscr{L}$ of the stage can be obtained from Eqs. 11 and 14 by integration:

$$\mathscr{L} = \frac{L_{t(O)}(1 - \theta)\ln(r_O/r_I)}{2\pi N}\int_1^{1/(1-\theta)}\frac{dL'}{\sum_{i=1}^{m}\bar{P}^{*i}(x^i p_O - y^i p_I)} \tag{19}$$

The total capillary length is then $\mathscr{L}N$. A fourth-order Runge-Kutta computer program was used to determine the composition of the permeated product stream and the capillary length.

Another flow pattern in a permeation stage of interest to this study is the "perfect mixing" case. This case assumes that the composition of the high- and low-pressure streams at any point in the stage is the same as that of the corresponding product streams. This assumption is analogous to that made for a continuous-flow stirred tank reactor. The separation of multicomponent gas mixtures in a perfectly mixed permeation stage has been discussed (Huckins and Kammermeyer, 1953; Stern, 1972).

APPARATUS AND EXPERIMENTAL PROCEDURE

Permeability Measurements

Rates of permeation of pure krypton and xenon through silicone rubber capillaries were first measured over a range of temperatures and applied pressures. The apparatus used for these measurements has been described in a previous publication (Stern, Onorato, and Libove, 1977). The apparatus included a permeator device in the form of a shell-and-tube heat exchanger, which was constructed from a section of heavy wall Sch 80 PVC-I pipe. This pipe section formed the shell of the permeator; it was 0.914 m (36.0 in.) long and had an O.D. of 0.0254 m (1.0 in.). The shell contained a bundle of 263 silicone rubber capillaries, each with a nominal O.D. of 635 μm (0.025 in.) and a nominal I.D. of 305 μm (0.012 in.). The two ends of the bundle of capillaries were encased in 0.0635 m (2.5 in.)-thick tube sheets.

The procedure used to cast the tube sheets, which consisted of a three-layered "sandwich" of epoxy resin and silicone rubber sealant, has also been described. The length of capillaries exposed to the penetrant gases was 0.914 m (36.0 in.). The total permeation area was 0.480 m^2 (5.165 ft^2) and the membrane packing density was 4132 m^2/m^3 (1260 ft^2/ft^3). Talcum powder was sprayed on the external surface of the capillaries to allow the formation of flow paths for gases. The ends of the permeator were closed by means of two 0.0635 m (2.5 in.)-thick end caps made from the same material as the permeator shell. The shell was provided with an inlet for the high-pressure feed stream and outlets for the low-pressure (permeated) and high-pressure (unpermeated, or residue) product streams. The inlet and low-pressure outlet were located at the same end of the permeator so as to permit the gas streams inside and outside the capillaries to flow counter currently to each other.

To perform permeability measurements with pure gases, the gas of interest was admitted to the permeator at some desired constant pressure p_O. The silicone rubber capillaries in the permeator were pressurized externally, because this method of pressurization was found previously to be preferable to internal pressurization (Stern, Onorato, and Libove, 1977). The gas permeating through the capillary walls flowed inside the capillaries and through the low-pressure permeator outlet into a calibrated borosilicate buret, where the rate of permeation was measured by the water displacement method. The pressure inside the capillaries, p_I, was approximately atmospheric. The high-pressure outlet of the permeator was closed during measurements with pure gases.

Pressure Drop Measurements

Pressure drop measurements were performed to determine the allowable capillary-packing density in the permeator as well as the highest allowable pressure. These measurements were made by passing a stream of nitrogen gas through the permeator, on the outside of the capillaries. The gas pressure at the permeator inlet was varied from 2.39 $\times$ 10^5 N/m^2 (34.7 lb/in.^{2} abs) to 5.84 $\times$ 10^5 N/m^2 (84.7 lb/in.^{2} abs), but was maintained constant during each measurement. The flow rates of the low-pressure (permeated) and high-pressure (unpermeated) streams at the permeator outlets were measured by the water displacement method. Pressure drop measurements were made both outside and inside the capillaries, across the entire length of the permeator, by means of two U-tube manometers. The manometer used to measure the small pressure drop outside the capil-

TABLE 1. GAS PURITIES.

Gas	Grade	Purity, vol %	Suppliers
Krypton	Research	99.995	Matheson Co.
Xenon	Research	99.995	Matheson Co.

laries was filled with a manometric fluid with a specific gravity of 1.75, while the manometer employed to determine the much larger pressure drop inside the capillaries was filled with mercury.

Gas Separation Measurements

The above apparatus was employed also for gas separation studies with a Kr-Xe-O_2-N_2 mixture at several pressures and temperatures. The silicone rubber capillaries were pressurized externally, or shell-side, and the flow of the permeated and unpermeated gas streams was countercurrent. The flow rates of the two streams were measured by the water displacement method.

The compositions of the permeated and unpermeated streams were analyzed with a Beckman GC-5 gas chromatograph obtained from Beckman Instruments, Inc., of Fullerton, Ca. The gas mixtures were separated for analysis by means of a chromatographic column which was 5.5 m (18 ft) long and 0.00476 m (0.1875 in.) in O.D., and was filled with Linde 13X Molecular Sieve (Purer, 1965). The column was operated initially at −68°C for the best separation of oxygen, nitrogen, and krypton, and then at 50°C for the separation of xenon. The detector used was a thermal conductivity cell, which was operated at 150°C and 250 mA.

MATERIALS

Capillaries

The silicone rubber capillaries were manufactured by Dow Corning Corp. of Midland, Mich., and were designated as "Silastic Medical-Grade Tubing." The filler content of the silicone rubber was stated by the manufacturer to be 32.25 ± 3 vol% (51.66 wt%). The density of the polymer was 9.8×10^2 kg/m^3 (61.2 lb/ft^3), and that of silica filler was 2.2×10^3 kg/m^3 (137.3 lb/ft^3).

The nominal O.D. and I.D. of the capillaries were 635 μm (2.5×10^{-2} in.) and 305 μm (1.2×10^{-3} in.), respectively.* To check these nominal values, the O.D. and I.D. were measured by microscopic observations, and the I.D. was also determined more accurately from the weight of mercury required to fill a selected length of capillary. The measured outer and inner diameters of the capillaries were found to be very close to their nominal values (Stern, Onorato, and Libove, 1977). Consequently, the permeation area and packing density reported in the previous section are based on the nominal dimensions of the capillaries.

Gases

The pure gases used in the permeability measurements are listed in Table 1.

The quaternary gas mixture used in the separation studies was supplied by Air Products and Chemicals, Inc., of Tamaqua, Pa. The following analysis of the mixture was provided by the suppliers:

Krypton:	0.489 vol-%
Xenon:	0.507 vol-%
Oxygen:	21.9 vol-%
Nitrogen:	balance

* These capillaries were called "hollow fibers" in an earlier publication (Stern, Onorato, and Libove, 1977), but the former designation appears more suitable (Thorman and Hwang, 1978).

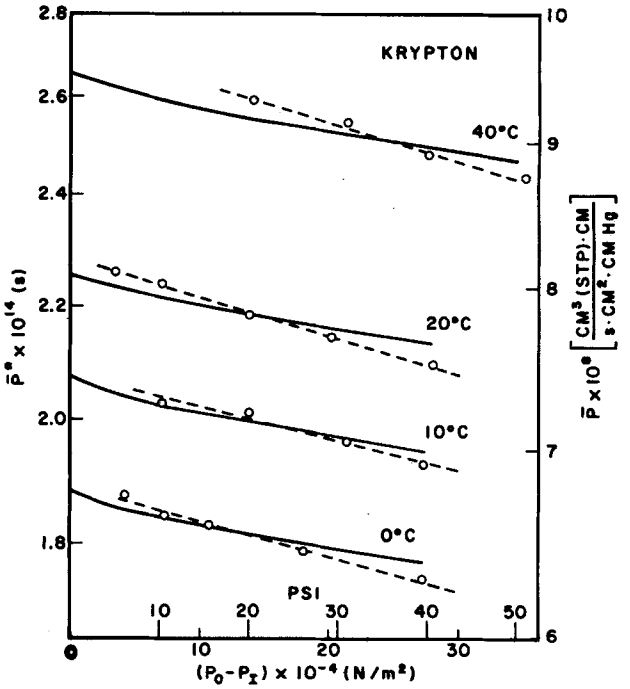

Figure 2. Effective permeability coefficient for Kr as a function of pressure difference across capillary wall.

EXPERIMENTAL RESULTS

Permeability Measurements

Rates of permeation of krypton and xenon through silicone rubber capillaries were measured at temperatures from 0 to 40°C and at pressure differences across the capillary walls ($\Delta p = p_o - p_l$) of up to 3.45×10^5N/m^2(50 psi). The pressure p_o was varied, whereas p_l was maintained constant at about 1×10^5 N/m^2 (14.7 lb/in.^{2} abs). The experimental results are given by the small circles in Figures 2 and 3. These results are expressed in terms of an effective permeability coefficient $\bar{P}^*$ defined by:

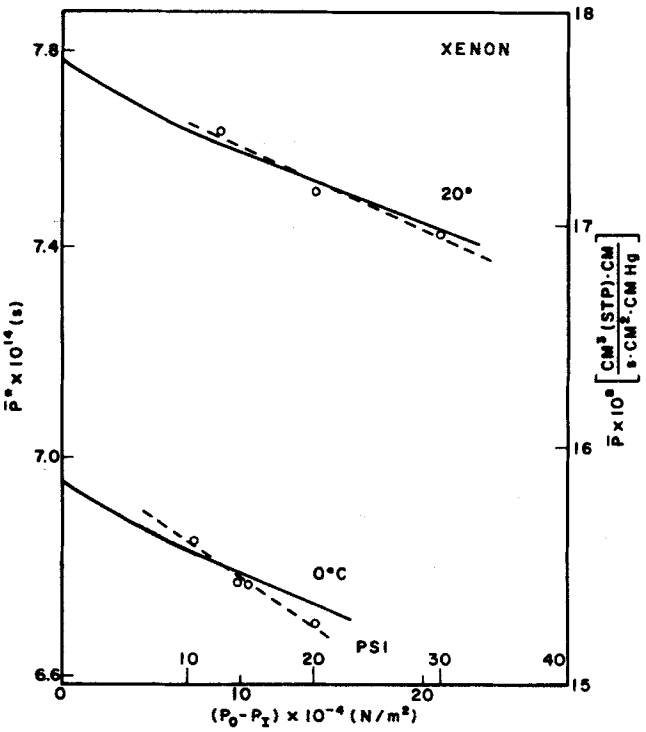

Figure 3. Effective permeability coefficient for Xe as a function of pressure difference across capillary wall.

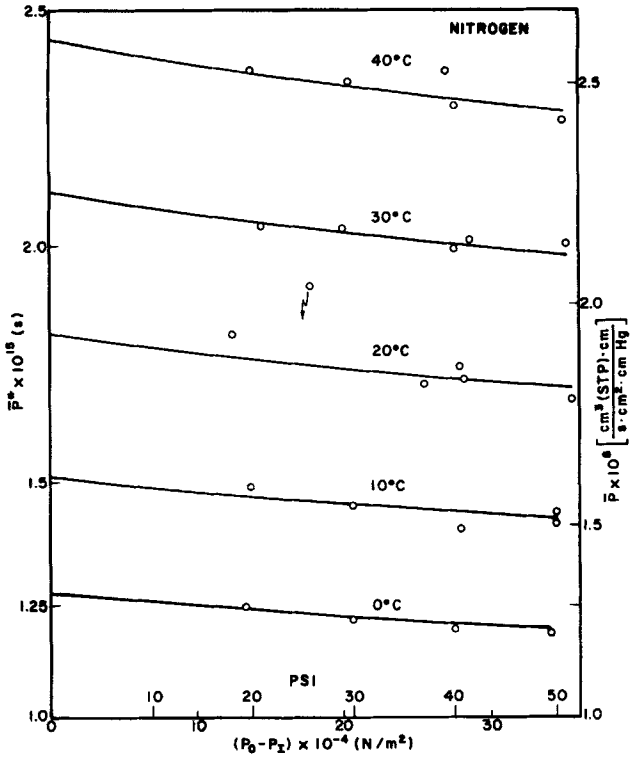

Figure 4. Effective permeability coefficient for N_2 as a function of pressure difference across capillary wall.

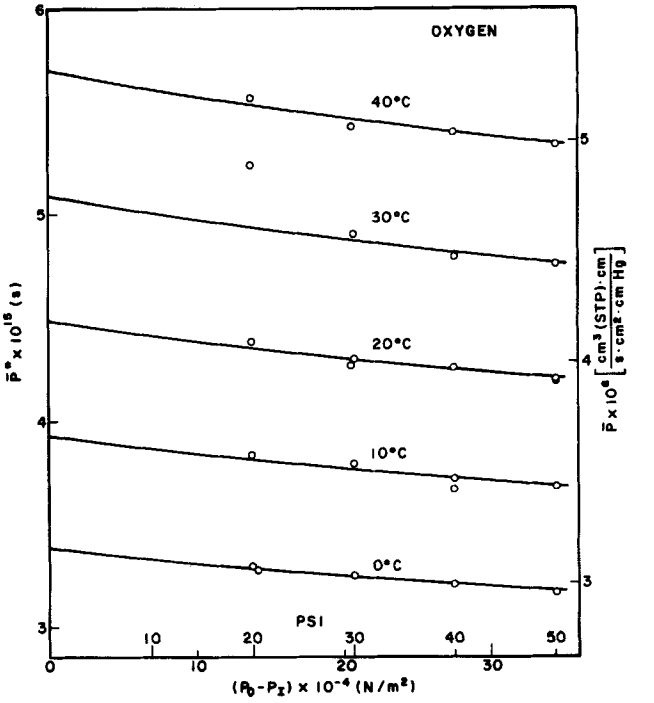

Figure 5. Effective permeability coefficient for O_2 as a function of pressure difference across capillary wall.

$$G = \bar{P}^* \frac{2\pi\ell(p_o - p_l)}{\ln(r_o/r_l)}, \tag{20}$$

where ℓ, r_o, and r_l are the length, outer radius, and inner radius, respectively, of the unstressed fibers ($\Delta p = 0$); $\ell = 0.914$ m (36.0 in .), and $r_o/r_l = 0.48$. The SI units of $\bar{P}^*$ are kg · m/(s · m² · Pa),, or *seconds*. Permeability coefficients have been customarily reported in the literature in units of cm³ (STP) · cm/(s · cm² · cmHg); these units should be multiplied by $3.3464 \times 10^{-9} M$, *where* M is the molecular weight of the penetrant gas, to obtain SI units. The maximum error in $\bar{P}^*$ has been estimated to be ±7%. Effective permeability coefficients are also shown for nitrogen and oxygen in Figures 4 and 5, respectively, as a function of Δp at several temperatures. These figures have been reported in a previous study (Stern, Libove, and Onorato, 1977) and are reproduced here for comparison with the data for krypton and xenon.

A comparison of Eqs. 2 and 3 shows that:

$$\bar{P}^* = \bar{P} f_1, \tag{21}$$

and this equation was used to plot the theoretical curves shown by the solid lines in Figures 2 to 5. The factor f_1 was calculated from Eqs. 4 to 7, assuming that the silicone rubber from which the capillaries were made was an isotropic incompressible material with a Young's modulus E of 3.09×10^6 N/m² (448 lb/in.²). Direct measurements actually showed the capillaries to be anisotropic with E having the values of 4.53×10^6 N/m² (657 lb/in.²) and 1.66×10^6 N/m² (240 lb/in.²) in the transverse and axial directions, respectively. The value of 3.09×10^6 N/m² used in calculating f_1 is thus an average of the values of E in the transverse and axial directions. Any possible dependence of E on temperature was neglected. The method used to obtain $\bar{P}$ in Eq. 21 has been discussed previously. Figures 2 and 5 shows that the calculated curves of $\bar{P}^*$ vs. $(p_o - p_l)$ provide a better fit of the measurements for nitrogen and oxygen than for krypton and xenon, although the agreement between theory and experiment is in all cases within the experimental error. To improve

TABLE 2. COMPARISON OF GAS PERMEABILITY MEASUREMENTS IN SILICONE RUBBER MEMBRANES.

Reference	Temperature, t(°C)	Permeability Coefficient, $\bar{P} \times 10^{15}$ [kg · m/(s · m² · Pa)][a] Xe	Kr	N_2	O_2	Filler Content	Remarks
Barrer and Chio (1965)	0	118.5	30.3	2.25	5.55	9.1 wt% Santocel CS (dens.: 1.66×10^3 Kg/m³); vol. fr.: 0.0554	Plane sheet, 2.06×10^{-3} m-thick (Imperial Chemical Ind., U.K.)
Barrer and Chio (1965)	0	103.0	28.8	1.91 (−0.8°C)	5.04	32.8 wt% Aerosil K3 Silica (dens.: 2.20×10^3 kg/m³); vol. fr.: 0.182	Tubing, 1.15×10^{-2} m O.D.X. 7.01×10^{-3} m I.D. (Midland Silicones U.K.)
This work[b]	0	99.9	27.3	1.83[c]	4.85[c]	51.7% Silica (dens.: 2.20×10^3 Kg/m³); vol. fr.: 0.3225	Capillaries, 6.35×10^{-4} m O.D. × 3.05×10^{-4} m I.D. (Silastic Medical Grade-Dow Corning Co.)

[a] Permeability coefficients were corrected for filler content by dividing $\bar{P}$ by the volume fraction of polymer.
[b] For unstressed fibers.
[c] From Stern, Onorato, and Libove (1977).

TABLE 3. COMPARISON OF ENERGIES OF ACTIVATION FOR GAS PERMEATION IN SILICONE RUBBER MEMBRANES.

Reference	Temperature-range, Δt(°C)	Energy of Activation E_p(kcal/kmol) Xe	Kr	N_2	O_2	Remarks
Barrer and Chio (1965)	0 to −37	670	1330	2600	2070	Plane sheet, 2.06×10^{-3} m thick (Imperial Chemical Ind., U.K.)
Barrer and Chio (1965)	0 to −40	1000	1590	3280	2590	Tubing, 11.5×10^{-3} m O.D. × 7.0×10^{-3} m I.D. (Midland Silicones, U.K.)
This work[a]	0 to 40	880[b]	1440	2800[c]	2210[c]	Capillaries, 6.35×10^{-4} m O.D. × 3.05×10^{-4} m I.D. (Silastic Medical Grade, Dow Corning Co.)

[a] Average values between 0 and 3.45×10^5 N/m² (50 psi) for unstressed fibers.
[b] For Δt from 0 to 20°C.
[c] From Stern, Onorato, and Libove, 1977.

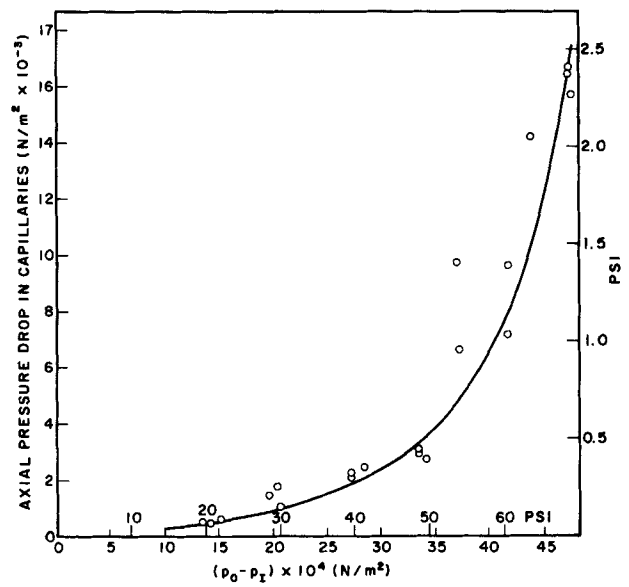

Figure 6. Axial pressure drop inside silicone rubber capillaries as a function of applied pressure.

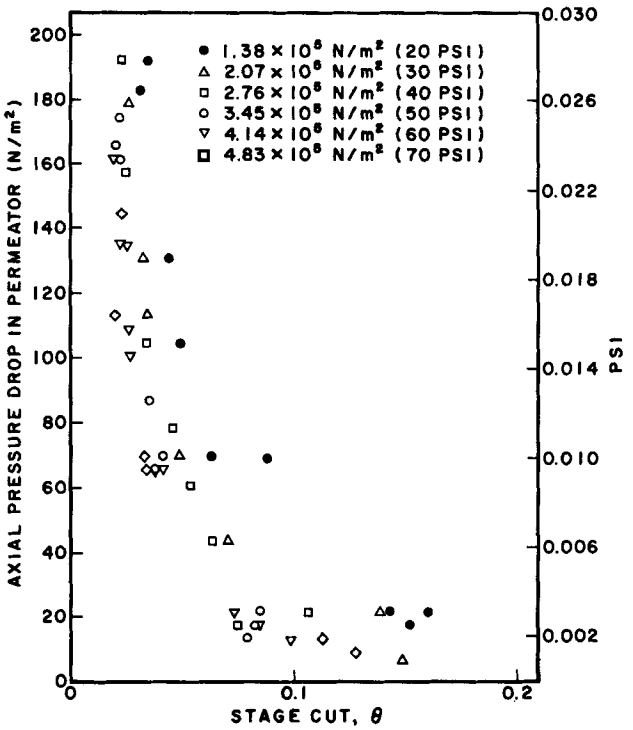

Figure 7. Axial pressure drop in permeator, outside silicone rubber capillaries, as a function of stage cut.

this agreement it may be necessary to modify the theory so as to account for the anisotropy of the capillary.

The most striking feature in Figures 2 to 5 is the decrease in the value of $\bar{P}^*$ with increasing Δp, at constant temperature. The above analysis suggests that this decrease is entirely due to the elastic deformation of the capillaries, at least at the pressures involved.

The dependence of the permeability coefficients for the unstressed fibers ($\Delta p = 0$) on temperature is given by the following relations:

$$\text{Krypton:} \quad \bar{P} \times 10^{15} = 318 \exp(-771/T) \tag{22}$$

$$\text{Xenon:} \quad \bar{P} \times 10^{15} = 340 \exp(-432/T) \tag{23}$$

$$\text{Nitrogen:} \quad \bar{P} \times 10^{15} = 221 \exp(-1410/T) \tag{24}$$

$$\text{Oxygen:} \quad \bar{P} \times 10^{15} = 198 \exp(-1111/T) \tag{25}$$

where $\bar{P}$ is in kg · m/(s · m² · Pa), or *seconds*, and T is in °K.

The permeability coefficients obtained in this work at 0°C are compared with the data of Barrer and Chio (1965) in Table 2. The latter were measured at low pressures; consequently, the values in Table 2 for the present work are for unstressed fibers. The values of $\bar{P}$ were also corrected for filler volume. Table 3 compares the energies of activation for permeation observed by Barrer and Chio (1965) with those obtained in the present study. The agreement between the two sets of data in Tables 2 and 3 is satisfactory, considering the differences in filler content, distribution, and particle size and shape.

Pressure Drop Measurements

The results of these measurements are shown in Figures 6 and 7. It is seen that the axial pressure drop both inside and outside the capillaries in the permeator was very small [2.1×10^3 N/m² (0.3 lb/in.²)] when the Δp across the capillary wall was less than about 2.76×10^5 N/m² (40 lb/in.²). Calculations confirmed that the axial pressure drop inside the capillaries is negligible under these conditions (Thorman and Hwang, 1978). When $\Delta p > 2.76 \times 10^5$ N/m², the axial pressure drop in the permeator outside the capillaries (shell-side) remained small, while a large axial pressure drop developed inside the capillaries (tube-side). The latter condition appears to have been caused by local collapses of the capillaries (pinching), probably at weak spots in the capillary walls, which impeded the gas flow. This effect was observed visually and recorded photographically in a permeator provided with a Plexiglass shell and built specially for this purpose. The effect was reversible: when Δp was reduced below about 2.76×10^5 N/m², the capillaries were seen to recover their original shape; i.e., the pinched areas disappeared. Thus, it does not appear practical to operate the permeator with the capillaries used in the present work at Δp's much above 3.45×10^5 N/m² (50 lb/in.²).

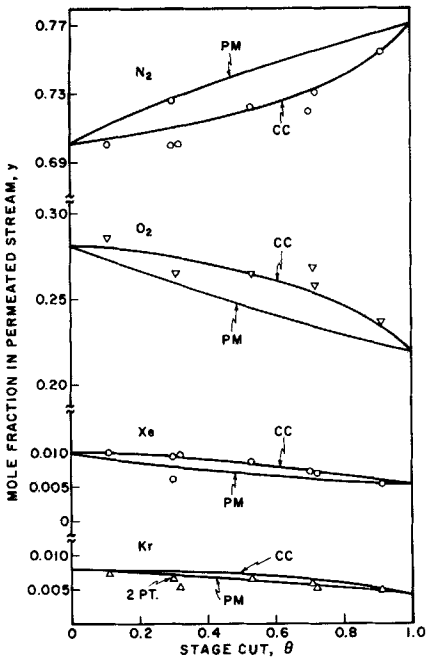

Figure 8. Separation of a Kr-Xe-O_2-N_2 mixture in a single permeation stage at 20°C and $\Delta p = 1.38 \times 10^5$ N/m^2 (20 lb/in.^{2}). Composition of permeated product stream as a function of stage cut (CC = countercurrent flow; PM = perfect mixing).

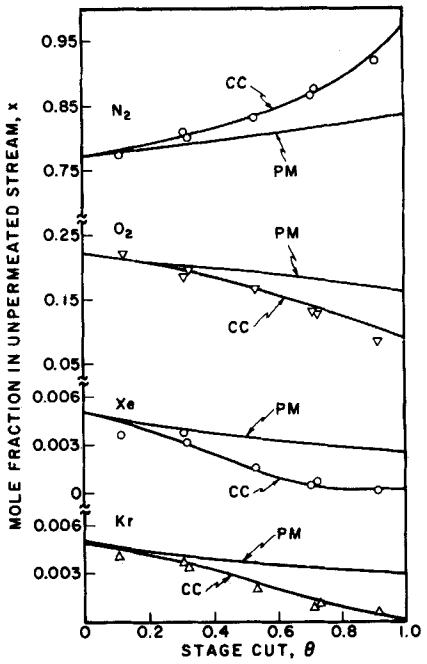

Figure 9. Separation of a Kr-Xe-O_2-N_2 mixture in a single permeation stage at 20°C and $\Delta p = 1.38 \times 10^5$ N/m^2 (20 lb/in.^{2}). Composition of unpermeated product stream as a function of stage cut (CC = countercurrent flow; PM = perfect mixing).

Gas Separation Measurements

The separation of a Kr-Xe-N_2-O_2 mixture in the capillary permeator was studied at pressure differences (Δp) of 1.38×10^5 N/m^2 (20 lb/in.^{2}), 2.07×10^5 N/m^2 (30 lb/in.^{2}), and 3.45×10^5 N/m^2 (50 lb/in.^{2}) and at the temperatures of -10 and 20°C. In all cases, the pressure inside the capillaries was about 1×10^5 N/m^2 (14.7 lb/in.^{2}). The composition of the gas mixture (0.489 vol-% Kr, 0.507 vol-% Xe, 21.9 vol-% O_2, and 77.1 vol-% N_2) was selected to illustrate the separation of small amounts of krypton and xenon from air. The oxygen and nitrogen concentrations were close to those in air; the concentration of oxygen in the mixture actually simulated the combined concentrations of oxygen and argon in air, since the effective permeability coefficients for these two gases in silicone rubber are very similar.

Typical experimental results are shown in Figures 8 to 15, where the compositions of the low-pressure (permeated) and high-pressure (unpermeated) product streams are given at several Δp's and temperatures. It can be seen that the permeate was enriched in krypton, xenon, and oxygen, and was depleted in nitrogen, by comparison to the feed gas. This behavior is particularly marked at stage cuts smaller than about 0.3.

The extent of separation of the Kr-Xe-O_2-N_2 mixture was also calculated on the basis of two theoretical models, namely, countercurrent flow and perfect mixing. It was assumed in these calculations that the effective permeability coefficients (P^{*i}) for the individual components of

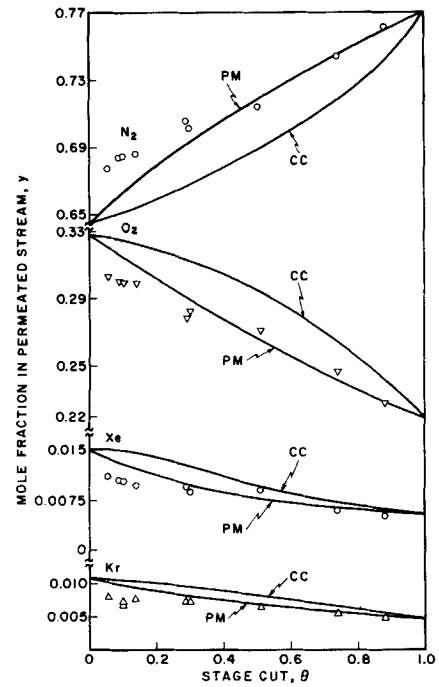

Figure 10. Separation of a Kr-Xe-O_2-N_2 mixture in a single permeation stage at 20°C and $\Delta p = 3.45 \times 10^5$ N/m^2 (50 lb/in.^{2}). Composition of permeated product stream as a function of stage cut (CC = countercurrent flow; PM = perfect mixing).

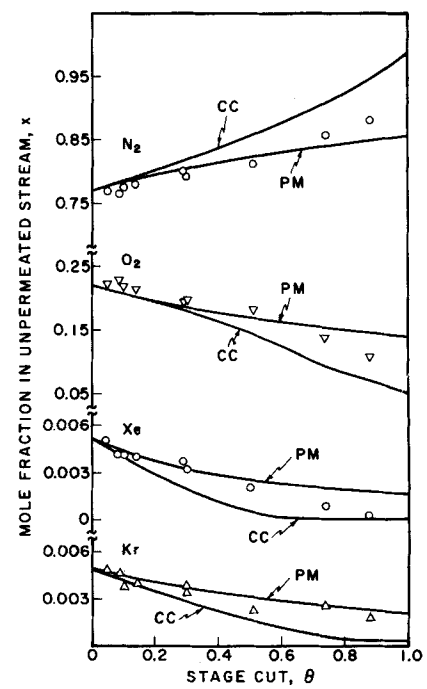

Figure 11. Separation of a Kr-Xe-O_2-N_2 mixture in a single permeation stage at 20°C and $\Delta p = 3.45 \times 10^5$ N/m^2 (50 lb/in.^{2}). Composition of unpermeated product stream as a function of stage cut (CC = countercurrent flow; PM = perfect mixing).

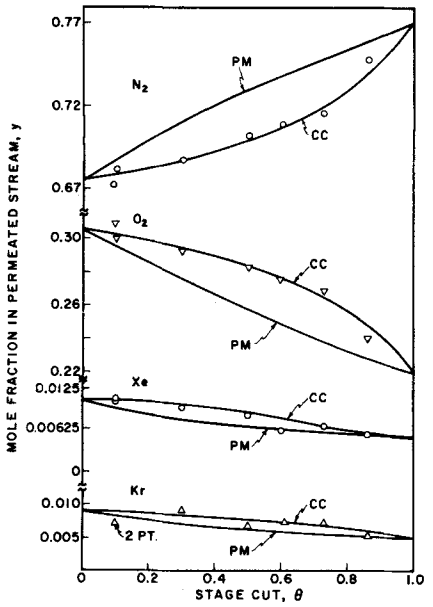

Figure 12. Separation of a Kr-Xe-O_2-N_2 mixture in a single permeation stage at -10°C and $\Delta p = 1.38 \times 10^5$ N/m^2(20 lb/in.^{2}). Composition of permeated product stream as a function of stage cut (CC = countercurrent flow; PM = perfect mixing).

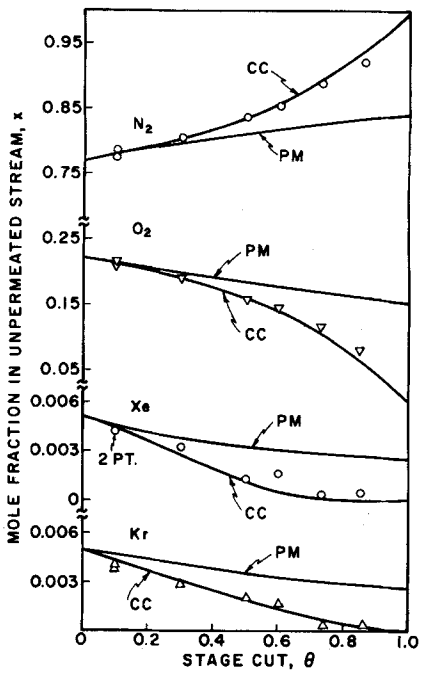

Figure 13. Separation of a Kr-Xe-O_2-N_2 mixture in a single permeation stage at -10°C and $\Delta p = 1.38 \times 10^5$ N/m^2 (20 lb/in.^{2}). Composition of unpermeated product stream as a function of stage cut (CC = countercurrent flow; PM = perfect mixing).

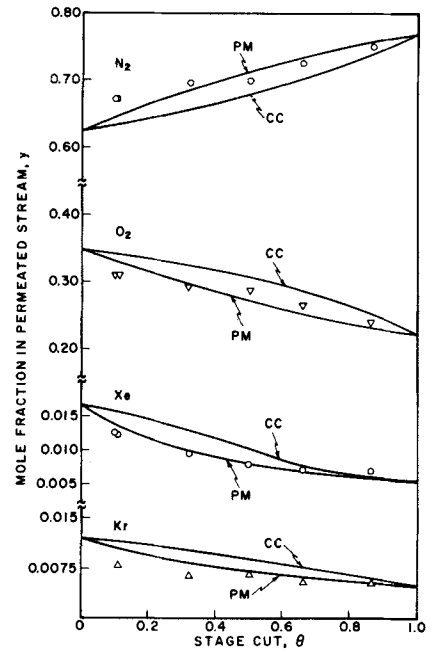

Figure 14. Separation of a Kr-Xe-O_2-N_2 mixture in a single permeation stage at -10°C and $\Delta p = 3.45 \times 10^5$ N/m^2 (50 lb/in.^{2}). Composition of permeated product stream as a function of stage cut (CC = countercurrent flow; PM = perfect mixing).

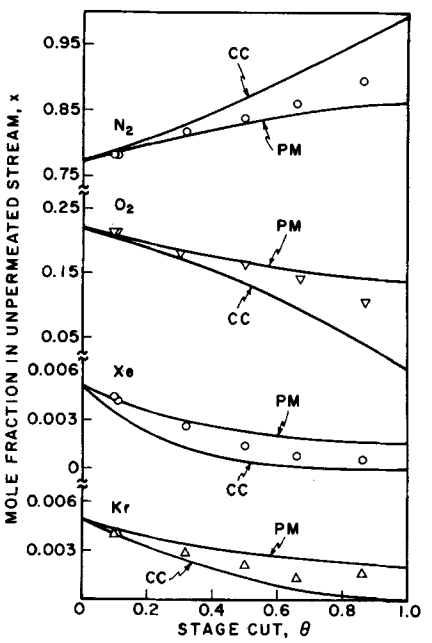

Figure 15. Separation of a Kr-Xe-O_2-N_2 mixture in a single permeation stage at -10°C and $\Delta p = 3.45 \times 10^5$ N/m^2 (50 lb/in.^{2}). Composition of unpermeated product stream as a function of stage cut (CC = countercurrent flow; PM = perfect mixing).

the mixture were the same as those for the pure components. The values of $\bar{P}^*$ for xenon at -10°C were obtained by extrapolation from higher temperatures. The theoretical results are indicated by the curves in Figures 9 to 15.

Most of the experimental data appear to fall close to the compositions predicted for countercurrent flow, the selected mode of permeator operation. However, at a Δp of 3.45×10^5 N/m^2 (50 lb/in.^{2}), the highest used in these measurements, the experimental data for stage cuts larger than 0.3 fall closer to the compositions predicted for the perfect mixing case. This change in the flow regime from countercurrent to perfect mixing probably was due to a pinching of the capillaries, as was evidenced also by the sharp increase in the axial pressure drop inside the capillaries at $\Delta p > \sim 2.76 \times 10^5$ N/m^2 (40 lb/in.^{2}). Figures 10 and 14 show that the experimental data for oxygen, xenon, and krypton fall below the theoretical curves for perfect mixing, and the data for nitrogen above these curves, at stage cuts smaller than 0.3. These discrepancies may be due to increased experimental error at low stage cuts.

The mechanism by which pinched capillaries affect the flow regime and separation in the permeator could be simply a decrease in the effective length of the capillaries. Only the section, or length, of capillary inside which permeated gas can flow unimpeded to the permeator outlet is useful for separation purposes; sections which are "pinched off" will contain essentially stagnant gas which does not participate in the separation process. Whatever the type of flow in the permeator, the extent of separation should approach that expected for perfect mixing as the effective capillary length is shortened. This effect becomes more pronounced as the pressure is raised and the capillaries collapse (i.e., are pinched) in an increasing number of spots. A previous study on the separation of air in a similar permeator (Stern, Onorato, and Libove,

1977) did not reveal such an effect because the permeator was operated in a cocurrent (not countercurrent) mode. It is known that the extent of separation in the case of cocurrent flow is close to that obtained with perfect mixing, particularly if the separation factor is small (Stern, 1972, 1976; Hwang and Kammermeyer, 1975); the separation factor for air (oxygen and nitrogen) in silicone rubber capillaries is only about 2.2.

The pinching of capillaries may have influenced also the permeability measurements with pure krypton and xenon, the more permeable gases in the present study. As is seen from Figures 2 and 3, the permeability coefficients for these gases decrease somewhat more rapidly with increasing pressure difference $p_o - p_I$ than predicted from theory, possibly because of the above effect. Measurements with oxygen and nitrogen, which are less permeable, appear to have been affected to a much smaller extent by the pinching effect.

The above studies were performed with stable isotopes of krypton and xenon, but the effects of radiation on silicone rubber must also be considered in view of the intended applications of the permeation processes. Rainey, Carter, and Blumkin (1971) as well as Ohno, Kakuta, et al. (1977) have investigated this problem and concluded that radiation exposure of silicone rubber membranes would not be a limiting factor in permeation cascades for the removal of radioactive krypton and xenon from nuclear reactor atmospheres.

ACKNOWLEDGMENT

The financial assistance of the Dept. of Energy, through its Div. of Basic Energy Sciences, is gratefully acknowledged. The authors are also grateful to Dr. W. J. Haubach and Prof. C. Libove for useful discussions and suggestions.

NOTATION

E = Young's modulus
E_p = energy of activation for permeation process
e_a = engineering principal strain in axial direction, in Eq. 5
f_1 = function defined by Eq. 4
G = total rate of gas permeation
L = local flow rate of high-pressure (unpermeated) stream outside the capillaries
L' = dimensionless variable defined by Eq. 14
$\mathscr{L}$ = length of single capillary, or of permeation stage
ℓ = length of single capillary in unstressed condition ($\Delta p = 0$)
m = number of components of a multicomponent mixture
N = number of capillaries in permeation stage
n = ratio of internal-to-external radii of unstressed capillary, r_I/r_O
P' = constant in Eq. 8
$\bar{P}$ = mean permeability coefficient for unstressed capillaries
$\bar{P}^*$ = effective permeability coefficient, $\bar{P}f_1$
p_O, p = gas pressure outside capillary (shell-side)
p_I = gas pressure inside capillary (tube-side)
p_r = ratio of pressures inside and outside a capillary, p_I/p_O
Q = contraction ratio of outer radius, R_O/r_O
q = contraction ratio of inner radius, R_I/r_I
R = universal gas constant
R_O = outer radius of stressed capillary
R_I = inner radius of stressed capillary
r_O = outer radius of unstressed capillary
r_I = inner radius of unstressed capillary
T = absolute temperature
x = mole fraction in high-pressure (unpermeated) stream
y = mole fraction in low-pressure (permeated) stream
z = axial direction in permeation stage
α_{ij} = ideal separation factor for component i relative to component j, $\bar{P}^{*i}/\bar{P}^{*j}$
Δp = pressure difference across capillary wall, $p_O - p_I$
θ = ratio of flow rate of low-pressure (permeated) product to feed flow rate, or "stage cut"

Superscripts

i = component of a multicomponent gas mixture
j = reference component

Subscripts

i = boundary of permeation stage at inlet of high-pressure (feed) stream
I = low-pressure side (tube-side)
o = boundary of permeation stage at outlet of high-pressure (product) stream
O = high-pressure side (shell-side)

LITERATURE CITED

Antonson, C. R., R. J. Gardner, C. F. King, and D. Y. Ko, "Analysis of Gas Separation by Permeation in Hollow Fibers," *Ind. Eng. Chem. Process Des. Develop.*, **16**, 463 (1977).

Barrer, R. M., and H. T. Chio, "Solution and Diffusion of Gases and Vapors in Silicone Rubber Membranes," *J. Polymer Sci.*, **C10**, 111 (1965).

Blaisdell, C. T., and K. Kammermeyer, "Gas Separation through Expansible Tubing," *AIChE J.*, **18**, 1015 (1972).

Blaisdell, C. T., and K. Kammermeyer, "Countercurrent and Cocurrent Gas Separation," *Chem. Eng. Sci.*, **28**, 1249 (1973).

Blumkin, S., et al., "Preliminary Results of Diffusion Membrane Studies for the Separation of Noble Gases from Reactor Accident Atmospheres," *Proceedings of the 9th Air Cleaning Conference*, Boston, Mass., **2**, 801-803, COF 660904 (Sept. 13, 1966).

Huckins, H. E., and K. Kammermeyer, "The Separation of Gases by Means of Porous Membranes," *Chem. Eng. Prog.*, **49**, 180 (1953); *ibid.*, **49**, 295 (1953).

Hwang, S.-T., and K. Kammermeyer, *Membranes in Separations*, Wiley-Interscience, New York (1975).

Kimura, S., T. Nomura, T. Miyauchi, and M. Ohno, "Separation of Rare Gases by Membranes," *Radiochem. Radioanal. Lett.*, **13**, 349 (1973).

Ohno, M., A. Kakuta, O. Ozaki, and T. Miyauchi, "Radiation Effects on Gas Permselective Membranes," *Radiochem. Radioanal. Lett.*, **26**, 291 (1976).

Ohno, M., T. Morisue, O. Ozaki, H. Heki, and T. Miyauchi, "Separation of Rare Gases by Membranes," *Radiochem. Radioanal. Lett.*, **27**, 299 (1976).

Ohno, M., O. Ozaki, and H. Sato, "Radioactive Rare Gas Separation Using a Separation Cell with Two Kinds of Membrane Differing in Gas Permeability Tendency," *J. Nucl. Sci. Technol.*, Japan, **14**, 589 (1977).

Ohno, M., A. Kakuta, O. Ozaki, S. Kimura, and T. Miyauchi, "Effects of Radiation on Gas Permselective Membranes," *J. Nucl. Sci. Technol.*, Japan, **14**, 673 (1977).

Ohno, M., T. Morisue, O. Ozaki, and T. Miyauchi, "Comparison of Gas Membrane Separation Cascades Using Conventional Separation Cell and Two-Unit Separation Cells," *J. Nucl. Sci. Technol.*, Japan, **15**, 376 (1978a).

Ohno, M., T. Morisue, O. Ozaki, and T. Miyauchi, "Gas Separation Performance of Tapered Cascade with Membrane," *J. Nucl. Sci. Technol.*, Japan, **15**, 411 (1978b).

Ohno, M., H. Heki, O. Ozaki, and T. Miyauchi, "Radioactive Rare Gas Separation Performance of a Two-Unit Series-Type Separation Cell," *J. Nucl. Sci. Technol.*, Japan, **15**, 668 (1978).

Purer, A., "Analysis of Impurities in Grade-A Helium in the ppb. Range," *J. Gas Chromatog.*, 3(5), 165 (1965).

Rainey, R. H., W. L. Carter, and S. Blumkin, "Evaluation of the Use of Permselective Membranes in the Nuclear Industry for Removing Radioactive Xenon and Krypton from Various Off-Gas Streams," Report ORNL-4522, Oak Ridge National Laboratory, Oak Ridge, Tenn. (April, 1971).

Stern, S. A., "Industrial Processing with Membranes," R. E. Lacey and S. Loeb, ed., Chapt. XIII, Wiley-Interscience, New York, 279-339 (1972).

Stern, S. A., "Membrane Separation Processes," P. Meares, ed., Chapt. 8, Elsevier Scientific Publishing Co., New York, 295-326 (1976).

Thorman, J. M. and S.-T. Hwang, "Compressible Flow in Permeable Capillaries under Deformation," *Chem. Eng. Sci.*, **33**, 15 (1978).

Walawender, W. P., and S. A. Stern, "Analysis of Membrane Separation Parameters: II. Countercurrent and Cocurrent Flow in a Single Permeation Stage," *Separation Sci.*, **7**, 553 (1972).

Manuscript received May 10, 1978; revision received April 16, and accepted April 30, 1980.